Structural Basis for a Bimodal Allosteric Mechanism of General Anesthetic Modulation in Pentameric Ligand-Gated Ion Channels

Zaineb Fourati, Rebecca J. Howard, Stephanie A Heusser, Haidai Hu, Reinis Ruza, Ludovic Sauguet, Erik Lindahl, Marc Delarue

▶ **To cite this version:**

Structural Basis for a Bimodal Allosteric Mechanism of General Anesthetic Modulation in Pentameric Ligand-Gated Ion Channels

Graphical Abstract

Anesthetic bimodal allosteric modulation
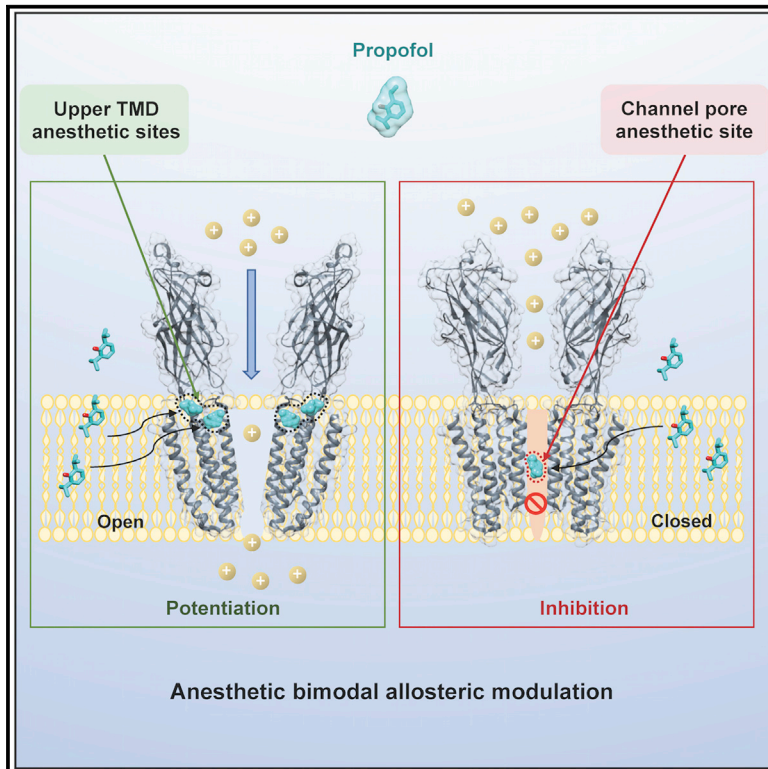
Authors

Zaineb Fourati, Rebecca J. Howard,
Stephanie A. Heusser, ...,
Ludovic Sauguet, Erik Lindahl,
Marc Delarue

Correspondence

delarue@pasteur.fr

In Brief

General anesthetics can both potentiate and inhibit pentameric ligand-gated ion channels, yet the structural basis for their effects remains unclear. Ten crystal structures and associated electrophysiology data by Fourati et al. point to a unified allosteric model for positive and negative modulation, providing a framework for structure-inspired drug design.

Highlights

- pLGICs are key targets for general anesthetics in the eukaryotic nervous system

- Propofol inhibits pLGICs by allosterically stabilizing the closed ion channel pore

- Mutations at the subunit interface enable propofol binding and potentiation

- Sites within each subunit provide an alternative mechanism of anesthetic potentiation

Data and Software Availability

5NKJ
6EMX
5NJY
5MZR
5MZT
5MVN
5MZQ
5MUR
5MVM
5MU0

CellPress

Structural Basis for a Bimodal Allosteric Mechanism of General Anesthetic Modulation in Pentameric Ligand-Gated Ion Channels

Zaineb Fourati,[1,5] Rebecca J. Howard,[2,5] Stephanie A. Heusser,[2] Haidai Hu,[1,3] Reinis R. Ruza,[1] Ludovic Sauguet,[1] Erik Lindahl,[2,4,6] and Marc Delarue[1,6,7,*]

[1]Unit of Structural Dynamics of Macromolecules, Institut Pasteur and UMR 3528 du CNRS, 75015 Paris, France
[2]Department of Biochemistry and Biophysics and Science for Life Laboratory, Stockholm University, 17165 Solna, Sweden
[3]Sorbonne Universités, UPMC University Paris 6, 75005 Paris, France
[4]Swedish e-Science Research Center, KTH Royal Institute of Technology, 11428 Stockholm, Sweden
[5]These authors contributed equally
[6]Senior author
[7]Lead Contact
*Correspondence: delarue@pasteur.fr
https://doi.org/10.1016/j.celrep.2018.03.108

SUMMARY

Ion channel modulation by general anesthetics is a vital pharmacological process with implications for receptor biophysics and drug development. Functional studies have implicated conserved sites of both potentiation and inhibition in pentameric ligand-gated ion channels, but a detailed structural mechanism for these bimodal effects is lacking. The prokaryotic model protein GLIC recapitulates anesthetic modulation of human ion channels, and it is accessible to structure determination in both apparent open and closed states. Here, we report ten X-ray structures and electrophysiological characterization of GLIC variants in the presence and absence of general anesthetics, including the surgical agent propofol. We show that general anesthetics can allosterically favor closed channels by binding in the pore or favor open channels via various subsites in the transmembrane domain. Our results support an integrated, multi-site mechanism for allosteric modulation, and they provide atomic details of both potentiation and inhibition by one of the most common general anesthetics.

INTRODUCTION

The family of Cys-loop receptors, known more generally as pentameric ligand-gated ion channels (pLGICs), has provided valuable insights into protein allostery for over 50 years (Changeux and Christopoulos, 2016). These proteins translate chemical signals—often synaptic neurotransmitters—into electrical signals by allosterically coupling extracellular ligand binding to the opening of a membrane-spanning, ion-selective pore (Figure 1) (Nys et al., 2013). Allosteric interactions further enable modulation of pLGICs by numerous drugs, including general anesthetics (Howard et al., 2014). Used to reversibly ablate consciousness,

memory, movement, and pain, these widely used agents are usually small, hydrophobic molecules exhibiting a wide range of molecular structures, likely targeting multiple receptor sites (Franks, 2006). A clear mechanistic understanding of pLGIC interactions with general anesthetics could unlock key principles of ion channel gating and modulation, and it could aid in the development of more potent and targeted modulators, including general anesthetics.

A complicating factor in structure-function studies of general anesthetics is their evident capacity to modulate pLGICs in at least two ways. In one branch of this channel family, type A γ-aminobutyric acid (GABA$_A$) and glycine receptors selectively conduct chloride anions, generally with the effect of hyperpolarizing membranes and reducing neuronal excitability; in another branch, activation of cation-conducting nicotinic acetylcholine (nACh) and type 3 serotonin (5-HT$_3$) receptors depolarizes neurons (Smart and Paoletti, 2012). General anesthetics *potentiate* many GABA$_A$ and glycine receptors, increasing chloride influx to dampen neuronal excitability; in addition, many anesthetics *inhibit* nACh receptors, decreasing cation flux to again limit firing (Flood et al., 1997; Violet et al., 1997). Specific channel subtypes or drugs may produce even more complex responses, for example, GABA$_A$ receptors containing the atypical ρ subunit exhibit general anesthetic inhibition rather than potentiation; conversely, nACh and 5-HT$_3$ receptors can be potentiated by some anesthetizing agents, such as ethanol (Howard et al., 2014). Given the conserved topology and, in many regions, amino acid sequences of pLGICs (Figure S1), it is plausible that anesthetic binding sites are also conserved among family members. Clearly, a complete mechanistic model must explain the capacity of these drugs to both potentiate and inhibit receptor function, either via shared or distinct sites of action.

Although pharmacological and biochemical studies have implicated a range of pLGIC sites in direct and indirect effects of general anesthetics (Olsen et al., 2014), the development of detailed mechanistic models has been limited by scarce structural data. The X-ray structure of a human GABA$_A$ receptor was determined only four years ago (Miller and Aricescu,
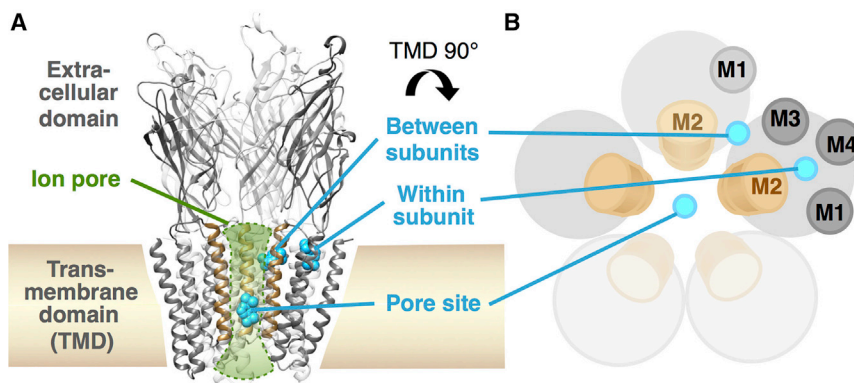
Figure 1. Proposed Sites of General Anesthetic Modulation in the Pore and Upper TMD of Pentameric Ligand-Gated Ion Channels

(A) Cut-away view from the membrane plane (brown) of a pLGIC (gray) including the M2 helices (tan), with two proximal subunits transparent to reveal the pore (green). Putative propofol positions are shown as spheres (cyan).

(B) Simplified cross-sectional model of the GLIC TMD, viewed from the extracellular side, showing M2 helices (tan) in each of the five subunits. TMD helices (gray) defining putative anesthetic sites (cyan) associated with the upper right subunit are labeled (M1–M4).

See also Figure S1.

2014), followed by representative human glycine (Huang et al., 2015) and nACh receptors (Morales-Perez et al., 2016). Along with related glutamate (Hibbs and Gouaux, 2011), 5-HT₃ (Hassaine et al., 2014), and glycine receptors (Du et al., 2015) from other eukaryotes, these data confirmed many topological features and likely endpoints in gating. Still, it has proved challenging to capture eukaryotic pLGICs in the presence of small allosteric modulators or in the multiple states required to characterize a functional landscape.

As with other complex biomolecules, prokaryotic homologs offer useful model systems for exploring functional and structural properties of pLGICs, including their modulation by drugs. In particular, the proton (H^+)-gated cation channel GLIC is inhibited by pharmacologically relevant concentrations of general anesthetics, including the common surgical agent propofol (Weng et al., 2010). Furthermore, propofol inhibition can be reduced or reversed (Sauguet et al., 2013a; Heusser et al., 2013) by site-directed mutations in the GLIC transmembrane domain (TMD), recapitulating the multiple modes of anesthetic modulation exhibited by human pLGICs. GLIC has proven to be an accessible structural target, crystallizing in multiple conformations, including apparent open (Hilf and Dutzler, 2009; Bocquet et al., 2009) and closed states (Sauguet et al., 2014); although precise functional correlates of these conformations remain to be verified, we refer to them as such here. In addition, so-called *locally closed* structures have been obtained under activating conditions from several GLIC variants (Prevost et al., 2012; Gonzalez-Gutierrez et al., 2013): in these structures, the extracellular domain is comparable to that of the open form, while the TMD aligns with the resting-state channel. The locally closed conformation likely represents a short-lived gating intermediate, e.g. the *flip*, *primed*, or *pre-active* state (Menny et al., 2017; Lev et al., 2017), that can be preferentially stabilized by chemical crosslinks or point mutations. Independent of its relevance to gating, the locally closed structure closely matches the resting state in the TMD, but it can be obtained under more flexible crystallization conditions and to higher resolution (Laurent et al., 2016); thus, it constitutes an accessible structural template for the closed pLGIC pore.

The GLIC model system has provided structural, functional, and computational evidence for various allosteric interactions, some challenging to reconcile in a single mechanistic model. In certain GLIC variants, potentiation by ethanol and bromoform was associated with an intersubunit-binding site at the extracellular-facing (upper) end of the open-state TMD (Sauguet et al., 2013a) (Figure 1). In addition, inhibitory anesthetics, such as propofol, crystallized between upper TMD helices (M1–M4) of individual open-state subunits (Nury et al., 2011)—a seeming paradox, given that inhibitors should stabilize a nonconducting state. An alternative inhibitory site was subsequently identified for xenon (Sauguet et al., 2016) and barbiturates (Fourati et al., 2017) in the pore of locally closed variants; bromoform anomalous signal was observed in both the closed pore and intrasubunit site of one variant (2-21'), but it was too weak to be resolved in the latter position (Table S1) (Laurent et al., 2016). These results call for a reexamination of propofol binding in the context of a multi-site mechanism, whose characterization could profoundly impact allosteric modeling and drug development.

Adopting a classic Monod-Wyman-Changeux (MWC) model (e.g., Changeux, 2013a), allosteric modulation should correspond to (1) a receptor containing a small number of (pseudo-) symmetric subunits that (2) populate an equilibrium between at least two states, (3) the distribution of which is shifted by selective binding of modulator to the higher-affinity state, often at interfaces between subunits. The first two of these criteria have been thoroughly documented for GLIC, which (1) consists of five symmetric subunits (Bocquet et al., 2009; Hilf and Dutzler, 2009), and (2) has been shown to transition from closed to open states at low pH (Bocquet et al., 2007). In this work, we aim primarily to address criterion (3), exploring the structural basis for selective stabilization of open or closed states. To this end, we identify GLIC point mutants with altered functional sensitivities to general anesthetics, particularly propofol, and we determine their structures under comparable conditions. Our results include ten structures of GLIC variants bound in various combinations of three sites, each of which has been shown to contribute to general anesthetic modulation in pLGICs (Howard et al., 2014). To elucidate the functional relevance of each site, we build this structural evidence into a mechanism of bimodal modulation, in which general anesthetics can bind in the ion pore to allosterically stabilize its closure or within or between subunits in the upper TMD to potentiate channel activation. We find close interplay between general anesthetic sites and gating determinants in both the pore and upper TMD, providing a

testable multi-site structural rationale for differential gating and modulation.

RESULTS

Altering Electrostatic Contacts in M2 (N239C and H235Q) Enables Pore Opening by Anesthetics

In exploring possible gating mechanisms in the model protein GLIC, we noted a pattern of electrostatic interactions between the upper M2 helix and backbone carbonyls of neighboring helices, specific to apparent open structures (Figure 2A). For instance, at the subunit interface, residues N239 and E243 (M2 positions 15' and 19', counting from the intracellular side) were oriented toward a water molecule, capable of bridging hydrogen (H-) bonds with M1-N200 in the neighboring subunit (Figures S2A and S2B). Substitutions at E243 have been shown to prevent channel opening (Prevost et al., 2012; Sauguet et al., 2013a); however, in keeping with previous work (Ghosh et al., 2013), we found GLIC variant N239C to be functional, with reduced sensitivity to H^+ activation in *Xenopus* oocytes (Figure 2B; Table S1). At pH 4, a condition that produced submaximal activation in functional recordings, apo GLIC-N239C (Figure 2C; Table S2) corresponded to a locally closed state (Prevost et al., 2012), with a 0.78-Å root-mean-square deviation (RMSD) in the TMD compared to resting-state GLIC (PDB: 4NPQ; Figure S3) and most upper-TMD electrostatic interactions ablated (Figures 2C and S2). Similar to previous structures in both apparent open and locally closed states, all GLIC variants in this work crystallized in the C2 space group with one pentamer in the asymmetric unit; phases were determined by molecular replacement using both open and closed starting models, and further model refinement was based exclusively on diffraction data, including regular checks of statistical bias (Brünger, 1992) (Table S2).

Upon submaximal activation (EC_{10}), net effects of propofol and bromoform switched from inhibition to potentiation in GLIC-N239C (Figure 2B). Addition of propofol to this variant yielded only non-diffracting crystals; however, under conditions otherwise identical to the apo state, co-crystallization with bromoform produced an apparent open structure (TMD RMSD = 0.42 Å versus PDB: 4HFI; Figures 2D, S3, and S4A; Tables S1 and S2), including a characteristically expanded pore (dilated from 4.2- to 6.0-Å diameter at the 9' gate; Figure S3C). Compared to other open structures, the N239C substitution did not dramatically alter the size of the proximal cavity, changing side-chain volume less than 5% (Zamyatnin, 1972). The major effect was instead electrostatic, as position 239 lost its capacity to H-bond with the neighboring subunit (Figures 2A and S2B), and it formed alternative hydrophobic contacts within the subunit (Figure 2D). Residues H235 and E243 were oriented as in the wild-type (WT) structure, although the interfacial water bridging E243–N200 was not resolved. Indeed, despite comparable resolution, mean temperature (B-) factors for the bromoform complex were approximately double those of other open-state structures (Table S2), and few solvent molecules could be definitively assigned. Still, strong anomalous peaks (visible above 9 σ; Figure S4A) allowed unambiguous assignment of one bromoform molecule within each subunit, proximal to M3-T255 (<3.6 Å; Figure 2D). Surprisingly, an additional bromine

anomalous peak was found in the GLIC-N239C channel pore (Figures 2D and S4A). Visible to only ~5 σ, this density was weaker than in the intrasubunit sites; still, it defined a bromoform molecule approximately centered in the ion pathway, in contact (<3.8 Å) with three of the five S230 (6') residues. This position was superimposable with a stronger bromoform density, visible up to 10 σ, in previous locally closed structures (Laurent et al., 2016) (Table S1).

In addition to electrostatic interactions between M2 and the neighboring subunit, most open structures of GLIC contained a direct contact (<2.9 Å) between the Nε nitrogen of M2-H235 and the backbone oxygen of M3-I259 in the same subunit (Figures 2A and S2C). We therefore asked whether alterations at H235 might also influence GLIC gating and modulation. Indeed, the substitution H235Q decreased H^+ activation, nearly reproducing the pH dependence of GLIC-N239C (Figure 2B). Apo GLIC-H235Q also crystallized at pH 4 in a locally closed state (Figures S3, S4B, and S4C; Tables S1 and S2). Furthermore, the H235Q mutation conferred potentiation by general anesthetics to an even greater degree than N239C (Figure 2B). Addition of either propofol (Figure 2E) or bromoform (Figures S4B and S4C) produced relatively well-diffracting crystals and structures in the apparent open state (Figure S3; Tables S1 and S2).

Similar to N239C, the mutated H235Q residue was not associated with a dramatic change in volume (Zamyatnin, 1972) or direct anesthetic contacts, but rather it influenced open-state electrostatic interactions. In place of the native contact between M2-H235 and M3-I259 (Figures 2A and S2C), the H235Q amide nitrogen contacted the sulfur atom of M1-M205 (<3.7 Å), to which it could donate an atypical H-bond (Figures 2E and S4C) (Gregoret et al., 1991). Within each M2 helix, another H-bond could be formed between H235Q and N239; this contact was associated with a reorientation of N239 toward H235Q and away from the subunit interface, further disrupting the WT electrostatic pattern (Figures 2E and S2). Propofol was resolved in four of the five subunits and made nonpolar contacts with residues in M1–M3 (Figure 2E). In the bromoform complex, multiple bromine peaks were visible in the anomalous map up to 9 σ, allowing identification of two ligands within each of the five subunits (Figures S4B and S4C). One subsite in each cavity was similar to the intrasubunit propofol site, coordinating with M1-I202 and M3-T255; a second subsite was proximal to M2-V242, in a pocket previously described as a *linking tunnel* between intra- and intersubunit regions (Nury et al., 2011; Laurent et al., 2016). Both subsites were partially occupied by bromoform in the previously determined WT complex (Sauguet et al., 2013a); in GLIC-H235Q, the second subsite was fully occupied.

Bulky Substitution in M1 (M205W) Stabilizes Open-State Intrasubunit Binding

To probe more direct determinants of general anesthetic modulation, we further investigated M1 residue M205, located at the lower perimeter of the intrasubunit-binding site (Figures 2D and 2E). As previously reported (Heusser et al., 2013), tryptophan substitution at this position (M205W) moderately reduced H^+ sensitivity and produced bimodal modulation: at moderate concentrations (10–100 μM), propofol had a net potentiating effect, while net inhibition was restored at higher concentrations
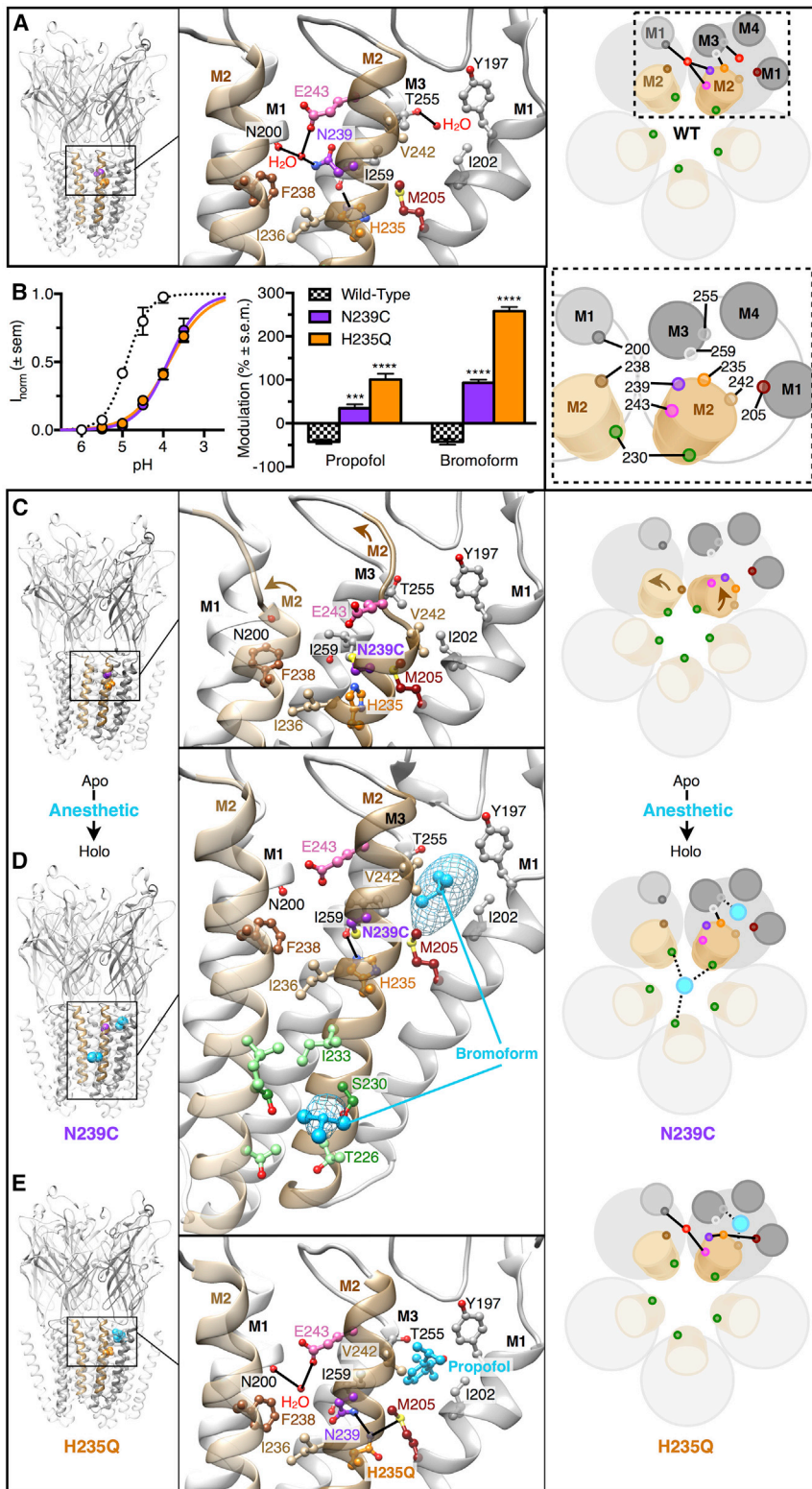
Figure 2. Altering Electrostatic Contacts (N239C and H235Q) Enables Pore Opening by Anesthetics

(A) Left: electrostatic-contact residues N239 and H235 mapped in WT GLIC under activating conditions (PDB: 4HFI), viewed from the membrane plane. Center: zoom view from the pore shows the upper TMD of two subunits. Residues associated with general anesthetic modulation are shown as balls and sticks, colored by heteroatom (N, blue; O, red; and S, yellow). Right: contact model of GLIC TMD in the apparent open state is viewed from the extracellular side, with putative mediators of anesthetic effects shown for the upper right subunit. In all panels, residues of interest are colored according to the key (box) as follows: M205, dark red; H235, orange; N239, purple; E243, pink; S230, green; V242, tan; N200, dark gray; T255, gray; and Y197, light gray. Black lines indicate possible H-bonds.

(B) Electrophysiology data showing reduced pH sensitivity (left) and reversed modulation of EC_{10} currents by 30 μM propofol and 1 mM bromoform (right) in GLIC-N239C (purple) and H235Q (orange) relative to WT (black). Data represent mean ± SEM; ***p < 0.001 and ****p < 0.0001.

(C) Representative apo structure of locally closed GLIC variants N239C and H235Q, shown in full (left), zoom (center), and contact model (right) views as in (A). Arrows in zoom and model views indicate channel opening.

(D) Views as in (A) of GLIC-N239C in the presence of bromoform. Mesh indicates bromine anomalous signal, contoured at 4 σ.

(E) Views as in (A) of GLIC-H235Q in the presence of propofol.

See also Figures S2–S4.
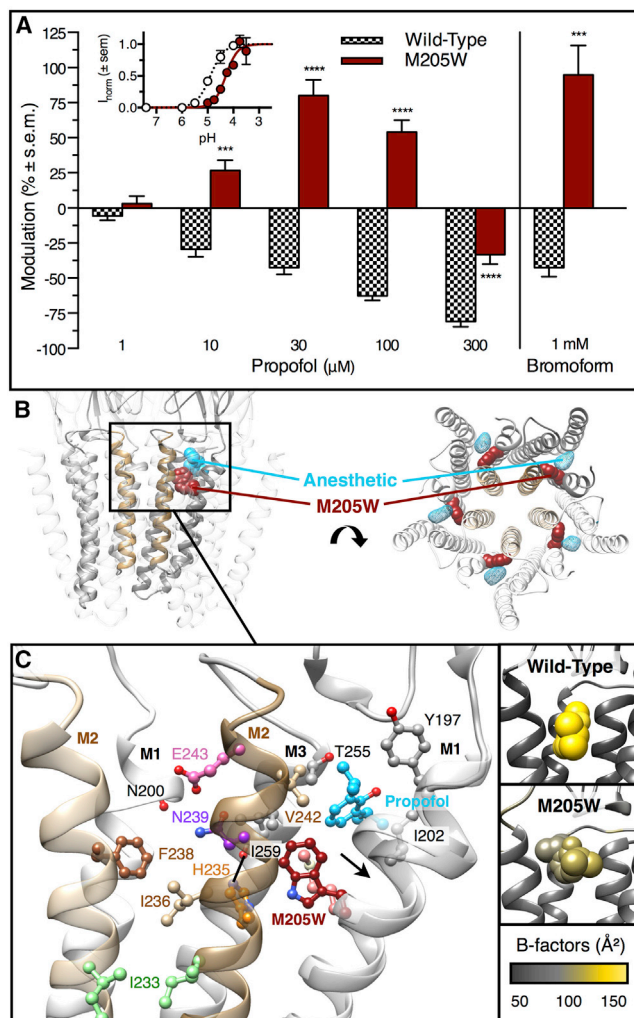
Figure 3. Bulky Substitution in M1 (M205W) Stabilizes Open-State Intrasubunit Binding

(A) Electrophysiology data showing activation (inset) and modulation of EC_{10} currents by a range of propofol concentrations (left) and 1 mM bromoform (right) in GLIC-M205W (burgundy) relative to WT (black). Data represent mean ± SEM; ***p < 0.001 and ****p < 0.0001.

(B) Left: GLIC-M205W TMD crystallized with propofol, viewed as in Figure 2A, showing M205W (burgundy) and propofol (cyan) associated with the right-hand distal subunit. Right: extracellular view of the bromoform complex shows the unmasked bromine anomalous map (cyan) contoured at 4 σ in all five subunits.

(C) Upper TMD of two GLIC-M205W subunits, viewed as in Figure 2A from the channel pore, with propofol and neighboring residues, including the mutated M205W, in ball-and-stick representation. For comparison, M1-M205 from the right subunit is superimposed from GLIC WT (PDB: 4HFI, arrow). Inset: equivalent views show WT (above) and M205W (below) structures, with propofol as spheres. Scale indicates B-factor color scheme.

See also Figures S2, S3, and S5.

(300 μM) (Figure 3A). Similar to moderate concentrations of propofol, the net effect of 1 mM bromoform was converted from inhibition to potentiation (Figure 3A). Although an apo structure could not be determined for GLIC-M205W, co-crystallization

with propofol or bromoform produced apparent open structures (Figures 3B and S3; Tables S1 and S2).

Despite the ∼40% increase in side-chain volume (Zamyatnin, 1972), the intrasubunit cavity was not blocked by M205W in either structure: instead, the upper M1 helix tilted away from M2 around the mutation (Figures 3C and S5), maintaining the potential for ligand binding. Indeed, in the propofol complex, strong peaks in the difference map were fit to propofol in four of the five subunits, proximal (<3.9 Å) to the mutated M205W (Figures 3B and 3C). Notably, B-factors for propofol were 26% lower in the mutant structure than in the WT complex (Nury et al., 2011) (Figure 3C), despite an increase in B-factors for the protein overall. In the bromoform complex, five distinct bromine peaks were visible up to 9 σ (Figure 3B); these allowed unambiguous assignment of a single bromoform molecule within each intrasubunit cavity, coordinated by I202 and T255 (Figure S5). In contrast to the multiple partially occupied bromoform sites in the WT complex (Sauguet et al., 2013a), the single bromoform site in each GLIC-M205W subunit was fully occupied, and side chains were rearranged such that M205W could donate an H-bond (<2.9 Å) to H235 in the same subunit (Figure S5).

Potentiation Corresponds to Interfacial Binding in F238A/N239A Variant

Looking beyond intrasubunit anesthetic binding, we investigated an alternative site at the upper-TMD subunit interface. Reducing steric hindrance in this region (by truncation of M2 position 14', F238A) was previously shown to switch the effect of small modulators, such as bromoform, from net inhibition to potentiation (Table S1). Accordingly, GLIC-F238A co-crystallized in the apparent open state, with bromoform partially occupying multiple sites within and between subunits (Sauguet et al., 2013a). The F238A mutant was generally insensitive to the larger agent propofol; however, further truncation of an adjacent asparagine (F238A/N239A) enabled potent propofol potentiation (Table S1) (Sauguet et al., 2013a). Here we sought direct evidence for propofol binding between subunits.

In the propofol-insensitive variant GLIC-F238A, co-crystallization in the apparent open state (Figure S3) enabled assignment of propofol to 2 of the 5 intrasubunit cavities (Figure 4A), in the site more extensively occupied in the H235Q and M205W variants (Figures 2E and 3B). In contrast, the double mutant F238A/N239A co-crystallized with propofol at all five subunit interfaces, filling the cavity vacated by the 239 side chain (Figure 4B; Tables S1 and S2). In place of water, the propofol hydroxyl group could bridge an extended H-bond between N200 and E243 in neighboring subunits (Figure S2A); propofol also made nonpolar contacts with the mutated F238A in one subunit and with residues, including N239A, in the other (Figure 4B). Propofol was not resolved in the intrasubunit site, and it was replaced by a water molecule proximal to T255. In the absence of propofol, the double mutant yielded only non-diffracting crystals.

Propofol Binds at the 6' Level in a Closed State of the GLIC Pore

Having identified propofol at multiple upper-TMD sites in the apparent open state, we asked whether the inhibitory effects of this ligand might correspond to selective binding in the closed
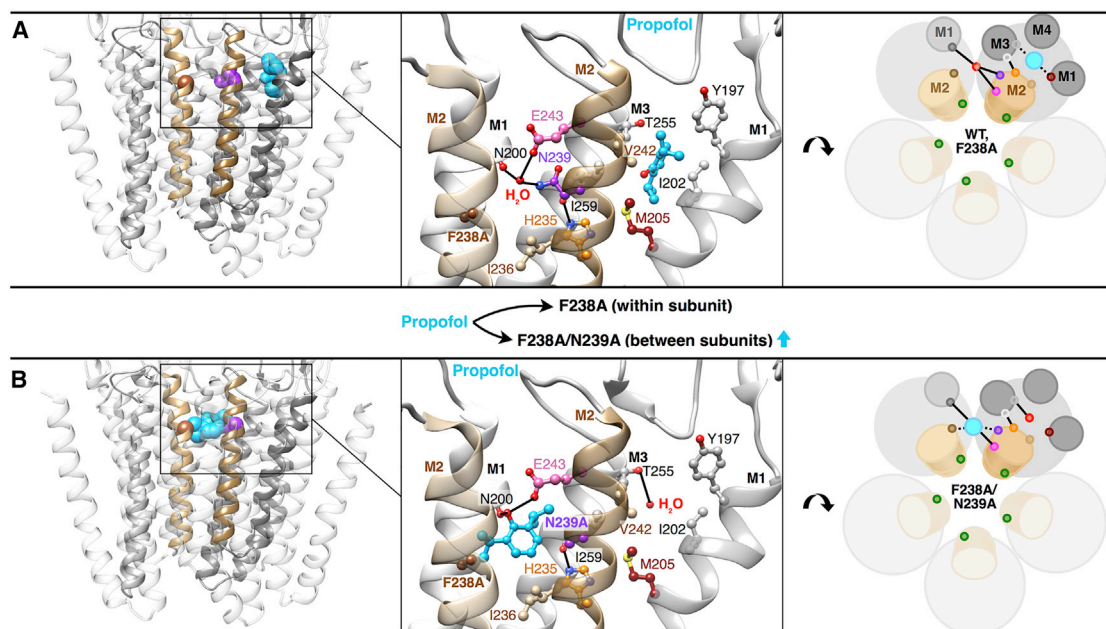
Figure 4. Potentiation Corresponds to Interfacial Binding in F238A/N239A Variant

(A) Left: GLIC-F238A viewed as in Figure 3B. Spheres indicate propofol (cyan) within the right distal subunit and F238A (brown) and N239 (purple) associated with the distal subunit interface. Center: zoom view shows two GLIC-F238A subunits, colored as in Figure 3C. Right: contact model for GLIC WT and F238A variants is shown.

(B) Views as in (A) of GLIC-F238A/N239A, with propofol at the subunit interface. Upward arrow indicates sensitivity to propofol potentiation.

See also Figures S2 and S3.

channel. To this end, we co-crystallized propofol with a GLIC variant (2-22′) in which a disulfide crosslink was shown to maintain a locally closed conformation (Prevost et al., 2012). Indeed, the propofol co-crystal structure of the crosslinked variant contained none of the open-state H-bonds described above (Figure S2), and it was superimposable with other locally closed structures (Figure S3), except for a single propofol molecule in the lower ion pore (Figures 5A and 5B; Tables S1 and S2). As seen in both closed (Prevost et al., 2012) and open apo structures (Sauguet et al., 2013b), detergent (presumably dodecyl-β-D-maltoside [DDM]) was observed in the pore above the 9′ gate; however, the lowermost detergent atoms terminated more than 4.7 Å from propofol, and they did not overlap or contact the pore site. We observed no density that could be assigned to propofol in the upper TMD or elsewhere.

Propofol was oriented with its long axis parallel to that of the channel, making nonpolar contacts with pore-facing residues at M2 positions 2′, 6′, and 9′ (T226, S230, and I233) (Figure 5B). In its orientation that best fits the electron density, the lone anesthetic molecule broke the 5-fold pseudosymmetry of the protein, placing its hydroxyl within 3.0 Å of S230 in chain B (Figure 5B). To probe the relevance of the pore-binding site in anesthetic modulation, we mutated S230 to threonine, its aligning residue in most human pLGICs (Figure S1). As previously reported (Sauguet et al., 2013b), channels containing this mutation expressed in oocytes; furthermore, upon increasing the reagent concentration and incubation time (3–7 ng cDNA for ≥ 6 days versus 0.5 ng WT cDNA for 2–3 days), they produced robust currents with H^+

sensitivity somewhat greater than WT (Figure 5C). At an equivalent (EC_{10}) level of activation, S230T also sensitized GLIC to inhibition by propofol or bromoform (Figure 5C; Table S1).

DISCUSSION

These structural and functional data support an allosteric mechanism for the modulation of pLGICs (Figure 6), including exchange between apparent closed (C) and open forms (O), with and without anesthetic bound in the channel pore ($_P$) or within ($_W$) or between ($_B$) subunits. To capture multiple states under comparable crystallographic conditions, representative structures were determined from GLIC point mutants associated with differing degrees of positive or negative modulation, in the presence of relatively concentrated modulators ($\sim$10-fold more than electrophysiology recordings). Caution should be taken in generalizing behavior from any one variant; furthermore, classification of data from multiple variants into binary functional states (C and O) likely obscures more subtle distinctions. Nonetheless, a preponderance of evidence from the ten structures and associated recordings in this work illustrates remarkable correspondence between functional gating and modulation in oocytes and relative stabilization of either the C or O states in crystallography. Figure S6 illustrates how each variant could produce the observed structure/function within the proposed framework, providing testable models for future study. Note that these figures depict only states (C_P, C_{PW}, O_{PW}, O_W, and O_B) evidenced by X-ray crystallography in known GLIC variants; alternative
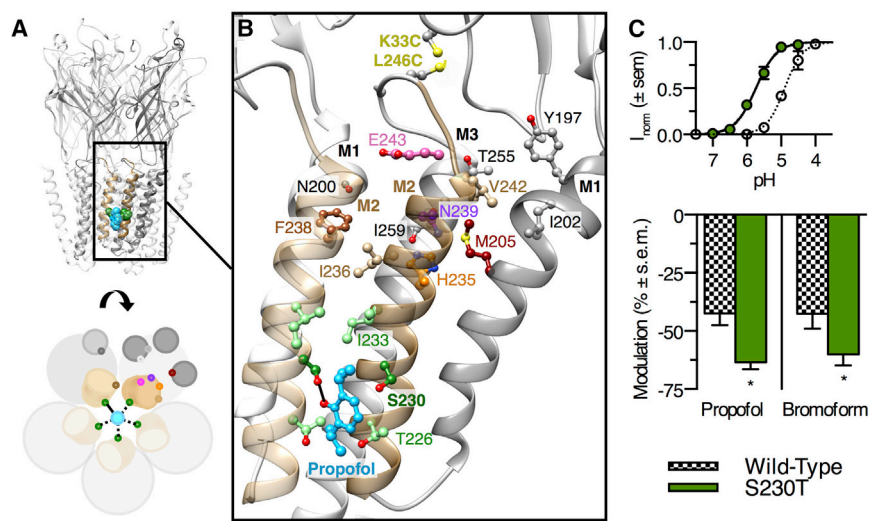
Figure 5. Propofol Binds at the 6' Level in a Closed State of the GLIC Pore

(A) Top: cut-away view of locally closed GLIC (2-22' variant) from the membrane plane; colors indicate M2 helices (tan) and propofol (cyan). Bottom: contact map as in Figure 4A shows propofol interactions with five S230 residues (green) in the closed pore.

(B) Zoom view as in (A), showing domain crosslink (K33C-L246C, yellow) and propofol (cyan) in the pore.

(C) Summary of two-electrode voltage-clamp recordings in oocytes showing enhanced gating (top) and inhibition of EC_{10} currents by 30 μM propofol and 1 mM bromoform (bottom) in GLIC WT (black) and S230T (green) variants. Data represent mean ± SEM; *p < 0.05.

See also Figures S2 and S3.

receptor or ligand geometries could enable further elaboration of this landscape.

Inhibition via Propofol Binding in the Closed Ion Pore

In the proposed mechanism (Figures 6 and S6A), exposure to agonist (in the case of GLIC, H^+) favors a conformational shift from state C to O. However, in the presence of general anesthetics, binding in the pore preferentially stabilizes a closed state (C_P), inhibiting function. The C_P state is not readily captured under standard GLIC crystallization conditions, which correspond to high activation and low inhibition (Howard et al., 2011); however, it could be trapped by covalent stabilization of the locally closed state (Figures 5A, 5B, and S6B). Pore binding appeared to be favored over other closed-state sites: anomalous bromine signal was detected in the intrasubunit site of one locally closed co-crystal structure (2-21', state C_{PW}), but it was substantially weaker than in the channel pore, precluding definitive assignment of intrasubunit ligands (Laurent et al., 2016).

In contrast, general anesthetics proved absent in the pore of 9 of 10 apparent open co-crystal structures (Figures 2E, 3B–3D, 4A, 4B, and S4C) (Nury et al., 2011; Sauguet et al., 2013a). The lone exception, GLIC-N239C (state O_{PW}), could represent a mode of open-pore block at high bromoform concentrations, possibly contributing to its lesser net potentiation relative to -H235Q (Figure 2B). Still, comparisons between this and other structures support a predominantly allosteric mechanism of inhibition. First, bromoform signal in the pore of locally closed complexes (Laurent et al., 2016) was consistently stronger than in the open GLIC-N239C pore, indicating higher affinity for the closed state. Second, bromoform signal in the GLIC-N239C pore was observed only in the context of stronger signal within all five intrasubunit sites (Figures 2D and S4A). These effects are in contrast to open-channel blockers, such as quaternary ammonium compounds and lidocaine, which crystallized exclusively in the open pore of WT GLIC (also proximal to S230; Hilf et al., 2010). Third, elevated B-factors in GLIC-N239C (Table S2) indicated the bromoform-occupied open pore to be relatively unstable, possibly poised to transition to a closed or intermediate state. In other

holo open-state structures, the more stably expanded pore appeared to disrupt pore binding more thoroughly, resulting in exclusive anomalous signal in the upper TMD (Figures S4B, S4C, and S5) (Sauguet et al., 2013a).

Propofol in the pore of locally closed GLIC overlapped previously identified poses of bromoform (Laurent et al., 2016), xenon (Sauguet et al., 2016), and barbiturates (Fourati et al., 2017), suggesting a conserved mechanism of inhibitory action. Unlike previous, distal gain-of-function mutations, which failed to alter anesthetic effects (Nury et al., 2011), the mutation S230T enhanced general anesthetic inhibition at an equivalent level of activation, consistent with relative stabilization of the C_P versus C states upon adding hydrophobic contacts in the pore. These findings validate previous free-energy perturbation studies, which predicted propofol to bind with micromolar affinity to the same region around S230 (LeBard et al., 2012). In addition, mutations at either end of this region have been shown to reduce propofol sensitivity (Tillman et al., 2013), possibly by limiting access via extra- or intracellular vestibules.

The pore-binding site for propofol further corresponds to inhibitory contacts implicated in a range of pLGICs. In nACh receptors, allosteric stabilization of closed channels via pore binding was proposed over 20 years ago (Bertrand et al., 1997); later, labeling studies showed propofol to interact with pore-facing residues in several subunits, particularly the 6' position (Jayakar et al., 2013). The equivalent site in α/β (Johnson et al., 2012) and ρ-type $GABA_A$ receptors (Borghese et al., 2016) also contributed an inhibitory component to n-alcohol modulation. In the bacterial homolog ELIC, co-crystal structures with bromoform (Spurny et al., 2013), ethanol (Chen et al., 2017), and isoflurane (Chen et al., 2015) showed closed-pore binding, in the latter cases at the 6' position; similar to our GLIC results, isoflurane appeared to stabilize the resting state of the pore and to inhibit more potently in the presence of threonine at 6'. Note that this model assumes negligible contributions from gating endpoints other than the apparent closed and open forms, for example, the desensitized state; although structural details are lacking for the desensitized structure of GLIC or its contribution to anesthetic
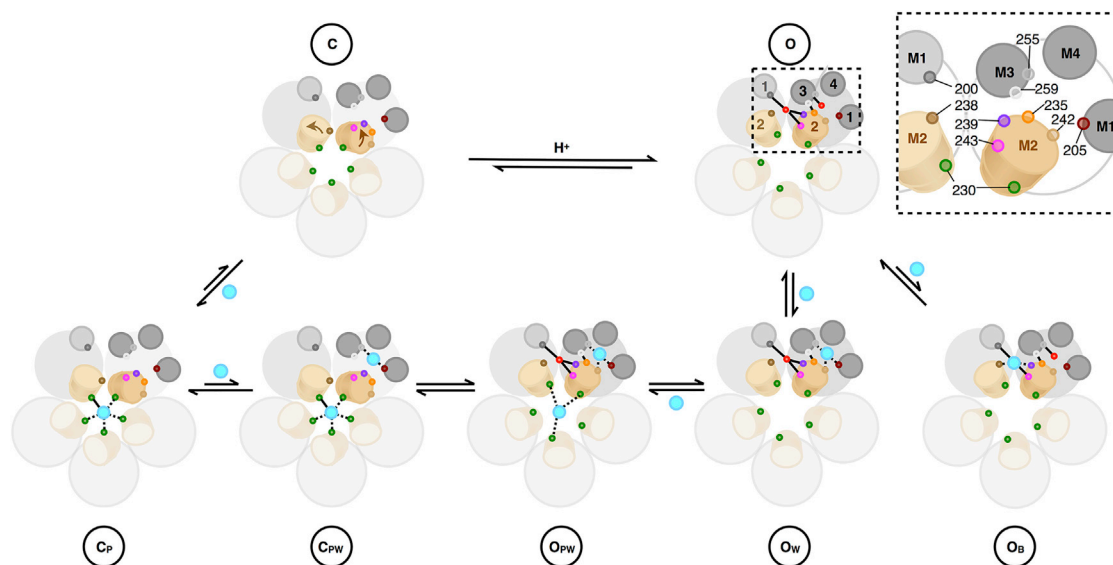
Figure 6. A Multi-site Mechanism for Bimodal Modulation of pLGICs

Top: protonation favors a conformational change from apparent closed (C) to open (O) states, associated with a tilt of the upper M2 helices away from the pore (arrows in C).

Bottom: holo states are classified by anesthetic binding in the channel pore ($_P$), within ($_W$) intrasubunit sites, or between ($_B$) subunits. Left to right: binding of anesthetic (cyan) in the channel pore is favored in the closed state (C_P), represented here by the crosslinked 2-22′ variant. Additional weak binding within each closed-state subunit (C_{PW}) is documented in some crosslinked channels (Laurent et al., 2016). Open-state binding within each subunit (O_W) is permitted in WT GLIC (Nury et al., 2011) and further stabilized in variants H235Q and M205W; additional, weaker binding in the open pore (O_{PW}) is documented in variant N239C. Binding between open-state subunits (O_B) is unfavorable for WT GLIC, though sterically allowed in GLIC-F238A (bromoform) and -F238A/N239A (propofol). Each model shows the five M2 helices (tan) plus additional helices of the upper right subunit and neighboring interface (gray). As defined in the key, colored circles represent anesthetic binding sites and key contacts implicated in anesthetic modulation for one subunit interface. Solid and dashed lines represent possible H-bonds and hydrophobic contacts, respectively. For clarity, upper-TMD-binding sites are indicated for only one subunit, although binding in up to five equivalent sites is expected.

See also Figure S6.

modulation, more complex models could be required for specific drug-receptor systems.

Potentiation via Propofol Binding at the Subunit Interface

Whereas WT GLIC is inhibited by general anesthetics, point mutations at the upper-TMD subunit interface enable its use as a model for potentiation. For instance, truncating the 14' side chain (F238A) allowed small modulators (ethanol and bromoform) to enhance channel function and to co-crystallize between subunits (Sauguet et al., 2013a). Here we showed binding of the larger modulator propofol in the same site upon truncating both 14' and 15' (F238A/N239A), corresponding to potent potentiation (Sauguet et al., 2013a). Thus, removing steric hindrance facilitated binding between subunits in the open state (Figure 6, state O_B), such that ligands could preferentially stabilize open channels and potentiate function (Figure S6C). We noted that this binding mode was associated with an increase in not only cavity volume (Sauguet et al., 2013a) but also intersubunit interaction: compared to the native water molecule found in this site (Figures 2A and 4A), propofol bridged a greater number of contacts between subunits (Figure 4B), potentially stabilizing the open state. The growth of high-quality GLIC-F238A/N239A crystals in the presence, but not the absence, of propofol further suggests binding was instrumental in promoting an ordered state of

the open channel. Indeed, except when directly perturbed, electrostatic interactions at this subunit interface were consistently and selectively found in open structures (Figures S2A and S2B).

Interfacial determinants of propofol potentiation in GLIC-F238A/N239A were consistent with prior observations in eukaryotic pLGICs. In general, GABA$_A$ and glycine receptors (which primarily exhibit anesthetic potentiation) contain smaller residues at 14' and 15' than nACh and 5-HT$_3$ receptors (which exhibit net anesthetic inhibition; Figure S1), consistent with subtype-specific binding. Labeling and docking studies have identified propofol at the GABA$_A$ receptor TMD interface (e.g., Bertaccini et al., 2013; Jayakar et al., 2014; and Yip et al., 2013), including specific contacts equivalent to GLIC N200 and F238 (Franks, 2015). In glycine receptors, an intersubunit crosslink equivalent to GLIC N200-E243 was also critical for gating; propofol potentiation was independent of this interaction (Lynagh et al., 2013), consistent with an anesthetic link between subunits in the open state. Functional studies further associated propofol potentiation in GABA$_A$ (Jurd et al., 2003; Stewart et al., 2014) and glycine receptors (Ahrens et al., 2008) as well as GLIC (Ghosh et al., 2013) with M2 position 15', which we validated here as a direct contact. Even in nACh receptors, photolabeling showed binding between subunits accounted for weak potentiating effects (Nirthanan et al., 2008). Thus, current evidence emphasizes a potentiating role for intersubunit binding, although, in principle, our

model could also accommodate inhibition by preferential stabilization of a nonconducting state (C$_B$); such a state has yet to be crystallized in GLIC, but it has been implicated in atypical effects on glycine (Lynagh and Laube, 2014) and GABA$_A$ receptors (Jayakar et al., 2015). Thus, the upper-TMD subunit interface appears to provide a fertile platform for allosteric modulation in a variety of pLGICs.

Potentiation via the Intrasubunit Cavity

In addition to verifying propofol potentiation via intersubunit binding, our results address the more controversial role of intrasubunit sites in the upper TMD. To our knowledge, the only prior propofol co-crystal structure with a membrane protein showed it binding within each subunit of open GLIC (Nury et al., 2011). Functional, computational, and labeling studies (Chiara et al., 2014; Tillman et al., 2013; Joseph and Mincer, 2016) further implicated this site in propofol modulation, even enabling the design of novel modulators (Gao et al., 2013; Heusser et al., 2013). Because propofol inhibits WT GLIC currents (Weng et al., 2010), the intrasubunit binding site was initially predicted to be inhibitory; however, this model did not clearly explain why it co-crystallized with GLIC in an apparent open state, especially as subsequent structures showed the intrasubunit site to be substantially remodeled in locally closed (Prevost et al., 2012) and resting states (Sauguet et al., 2014). In thiosulfonate-labeling studies, propofol failed to occupy either inter- or intrasubunit sites in the resting state (Ghosh et al., 2013); and we saw no intrasubunit propofol density in the locally closed complex (Figure 5), indicating its inhibitory interactions were mediated primarily by another region (i.e., the closed pore). As an alternative model, functional studies in GABA$_A$ (Wick et al., 1998) and nACh receptors (Arevalo et al., 2005) have suggested intrasubunit anesthetic binding contributes to channel potentiation, even in receptors exhibiting net inhibition.

Indeed, the present work identified multiple variants in which intrasubunit binding prefers the open state. In particular, intrasubunit anesthetic binding converted GLIC-H235Q and -N239C from locally closed to open forms under otherwise identical conditions (Figures 2C–2E), a rare example of a state change solely upon adding an allosteric modulator to an ion channel. Designed to destabilize the open state by disrupting key electrostatic contacts (Figure S2), the H235Q and N239C mutations indeed inhibited channel function (Figure 2B) and produced crystals in the locally closed state under apo conditions (Figures S6D and S6E); along with E243P (Prevost et al., 2012), T249A, and Y251A (Gonzalez-Gutierrez et al., 2013), these mutations define a growing series along the buried face of M2 and the M2-M3 loop associated with locally closed structures. Anesthetic binding within subunits of GLIC-H235Q and -N239C (Figure 6, state O$_W$) bridged alternative contacts (Figures 2D, 2E, and S4C), which appeared to compensate for apo open-state destabilization, enabling crystallization in the holo open state and potentiating channel function (Figures S6D and S6E).

Intrasubunit-bound structures in this work also offered a rationale for differential modulation of GLIC variants. Conformational stabilization of residue M205 in GLIC-H235Q could account for its relatively strong anesthetic binding and potentiation (Figures 2B, 2E, and S6D). In contrast, anesthetics bound GLIC-N239C

in both intrasubunit and pore sites (Figure 6, state O$_{PW}$) and exerted only moderate potentiation (Figure 2B), possibly arising from channel block or lesser relative stabilization of the open state (Figure S6E). In GLIC-M205W, functional data (Figure 3A), structural B-factors (Figure 3C), and occupancy (Figure S5), along with evident barriers to apo-state structure determination, further indicated that stabilization of anesthetics in the intrasubunit site could promote the O$_W$ state (Figure S6F). The bimodal profile of propofol modulation in GLIC-M205W (Figure 3A) provides further evidence for exchange between states bound in intrasubunit and pore sites: at high concentrations, propofol is predicted to saturate the intrasubunit sites and gain access to a lower-affinity site in the ion pore.

Conclusions

The analysis above supports a unified mechanism for both positive and negative modulation of pLGICs by general anesthetics (Figure 6). Addressing a key criterion for allosteric modulation (Changeux, 2013b), multiple structures in this work illustrate relative stabilization of the apparent open state upon modulator binding in the upper TMD, either switching the crystal conformation from closed to open (Figure 2) or enabling structure determination selectively in the holo form (Figures 3 and 4). Conversely, binding in the channel pore was shown in the closed state exclusively for propofol (Figure 5) and more strongly than in other states/sites for bromoform (Figure 2D) (Laurent et al., 2016), supporting a common inhibitory mechanism involving allosteric closure rather than solely channel block.

As a corollary to this criterion, modulators are often expected to bind at subunit interfaces, primed to influence the concerted transition between receptor states (Changeux and Christopoulos, 2016). Indeed, two of the modulation sites described in this work occupied such interfaces, either between subunit pairs in the upper TMD (Figure 4B) or bridging all five subunits in the channel pore (Figure 5A). In a third site, located within each subunit (Figures 2D, 2E, 3C, 4A, S4C, and S5), modulators mediated interhelical contacts specifically associated with the open state, again consistent with an allosteric mechanism. Thus, anesthetics can occupy multiple allosteric sites in pLGICs, each with distinct affinity and efficacy.

Whereas our work focuses on the highly accessible GLIC model system, each of these sites has been previously implicated in modulation of eukaryotic homologs (e.g., Howard et al., 2014) Thus, as previously shown for other receptors (Süel et al., 2003), allosteric modulation networks in pLGICs may be conserved through evolution. Notably, a detailed characterization of barbiturate modulation was recently accomplished in heteromeric GABA$_A$ receptors by integrating an allosteric co-agonist model with compensatory inhibition (Ziemba and Forman, 2016), echoing the bimodal effects modeled in this work. Similar phenomena have also been observed in voltage-gated potassium (Barber et al., 2011) and sodium channels (Barber et al., 2014), indicating that insights from pLGICs could provide relevant models for a variety of systems. An important ongoing task will be to quantify the parameters and applicability of the proposed mechanism in various drug-receptor systems, for example, by the analysis of molecular dynamics simulations based on these or related structural templates.

EXPERIMENTAL PROCEDURES

Reagents
Chemicals were purchased through VWR International or Sigma-Aldrich. Mutant cDNA constructs were generated using commercially synthesized primers and the GeneArt site-directed mutagenesis system (Thermo Fisher Scientific, Waltham, MA), confirmed by cycle sequencing (Eurofins Genomics, Ebersberg, Germany), and amplified by HiSpeed Midi plasmid preparation (QIAGEN, Germantown, MD). Propofol was dissolved in DMSO and stored as a 100-mM stock solution at 4°C.

Protein Purification and Crystallization
GLIC variants were expressed in a pET-20b-derived maltose binding protein (MBP)-fusion vector in C43 *Escherichia coli*, solubilized in DDM, and purified according to previous protocols (Bocquet et al., 2009; Sauguet et al., 2013b). Protein samples were mixed 1:1 with reservoir (100 mM acetate [pH 4], 400 mM sodium thiocyanate [NaSCN], 3% DMSO, 16% glycerol, and 12%–14.5% polyethylene glycol 4000 [PEG 4K]), microseeded with previous GLIC crystals, and grown by vapor diffusion in hanging drops at 18°C. For co-crystal structures, 2 mM propofol was added to the reservoir prior to setting drops or 20 mM bromoform was added after setting drops. Crystals appeared overnight, reached maximum dimensions after 1 week, and were collected on cryoloops, immediately flash-frozen, and stored in liquid nitrogen.

Crystallography
We collected single-crystal datasets on beamlines Proxima-I and Proxima-II at Synchrotron Soleil, as well as ID23 and ID29 at the European Synchrotron Radiation Facility. For crystals with bromoform, datasets were collected at the peak bromine wavelength (0.9191 Å) using the inversed-beam strategy to optimize the anomalous signal. Data were integrated with XDS (Kabsch, 2010) and further scaled using Aimless in the CCP4 suite (Collaborative Computational Project, Number 4, 1994). To obtain initial phases, previously determined structures of apo GLIC were used as starting models in Refmac5 (Murshudov et al., 2011). Models were refined using Buster (Blanc et al., 2004), with noncrystallographic symmetry restraints applied throughout, and validated using Molprobity (Davis et al., 2007) (Table S2). Pore diameter (Figure S2) was characterized using MOLEonline (Berka et al., 2012). TMD RMSDs (Figure S3) were calculated for protein Cα atoms in M1 (196–218), M2 (220–245), M3 (253–282), and M4 (284–315) using the Match-Align function in UCSF Chimera (Meng et al., 2006). All ligands were refined with full occupancy, except in GLIC-H235Q, where occupancies were first refined with Buster, then ligands were built with partial occupancies (0.7 for propofol and 0.5 for bromoform).

Activation
Isolated oocytes from female *Xenopus laevis* frogs were purchased (EcoCyte Bioscience, Dortmund, Germany), stored, injected, incubated, and clamped according to previous protocols (Heusser et al., 2016). Briefly, each oocyte was injected with 0.5–6.0 ng/32.2 nL GLIC cDNA in vector pMT3 and stored at 12°C for 2–12 days. Recordings were performed at −70 mV using an OC-725C voltage clamp (Warner Instruments, Hamden, CT) in running buffer (10 mM HEPES [pH 7.5–8.5], 123 mM NaCl, 10 mM sodium citrate, 2 mM KCl, 2 mM MgSO$_4$, and 2 mM CaCl$_2$) at a flow rate of 0.5–1.0 mL/min. Activation buffers contained 10 mM citrate in place of HEPES, adjusted to pH 3.5–6.5. Solutions were exchanged manually or via a VC3-8 pressurized perfusion system (ALA Scientific, Farmingdale, NY). Currents were digitized at a sampling rate of 5 kHz with an Axon CNS 1440A Digidata system using pCLAMP 10 (Molecular Devices, Sunnyvale, CA). Each data point represents 3–9 oocytes from ≥2 frogs. Activation currents were fit to sigmoidal concentration-response curves and normalized to the fitted maximal response using Prism 6 (GraphPad, La Jolla, CA).

Modulation
Drug effects were measured according to a protocol previously standardized for human and bacterial ion channels (Heusser et al., 2013). Oocytes were perfused with running buffer, and receptors were activated by a 1- to 2-min application of low-pH buffer sufficient to produce 10%–20% maximal current (e.g., pH 5.5 for WT GLIC; denoted EC_{10}). Modulators were pre-applied for

1 min (final DMSO ≤ 0.02%), then co-applied with EC_{10} buffer for 1–2 min. Recovery was verified by applying EC_{10} buffer again in the absence of modulator. To minimize anesthetic loss during perfusion, we prepared and sealed all solutions immediately before use, and we applied drugs via <10-cm polytetrafluoroethylene tubing. Modulation (%) was calculated relative to the mean of pre- and post-drug responses. Results were analyzed by unpaired t test.

DATA AND SOFTWARE AVAILABILITY

The accession numbers for the GLIC variant structures reported in this paper are PDB: 5NKJ (apo N239C), PDB:6EMX (N239C with bromoform), PDB:5NJY (apo H235Q), PDB:5MZR (H235Q with propofol), PDB:5MZT (H235Q with bromoform), PDB:5MVN (M205W with propofol), PDB:5MZQ (M205W with bromoform), PDB:5MUR (F238A with propofol), PDB:5MVM (F238A/N239A with propofol), and PDB:5MU0 (2-22' with propofol). See Table S1.

SUPPLEMENTAL INFORMATION

Supplemental Information includes six figures and two tables and can be found with this article online at https://doi.org/10.1016/j.celrep.2018.03.108.

AUTHOR CONTRIBUTIONS

Z.F., H.H., R.R.R., and L.S. carried out crystallographic experiments and analysis. R.J.H. and S.A.H. carried out functional experiments and analysis and prepared the figures. M.D. and E.L. supervised crystallographic and functional experiments, respectively. Z.F. and R.J.H. prepared original manuscript drafts; Z.F., R.J.H., S.A.H., E.L., and M.D. reviewed and edited the paper.

DECLARATION OF INTERESTS

The authors declare no competing interests.

REFERENCES

Ahrens, J., Leuwer, M., Stachura, S., Krampfl, K., Belelli, D., Lambert, J.J., and Haeseler, G. (2008). A transmembrane residue influences the interaction of propofol with the strychnine-sensitive glycine α1 and α1β receptor. Anesth. Analg. *107*, 1875–1883.

Arevalo, E., Chiara, D.C., Forman, S.A., Cohen, J.B., and Miller, K.W. (2005). Gating-enhanced accessibility of hydrophobic sites within the transmembrane region of the nicotinic acetylcholine receptor's δ-subunit. A time-resolved photolabeling study. J. Biol. Chem. *280*, 13631–13640.

Barber, A.F., Liang, Q., Amaral, C., Treptow, W., and Covarrubias, M. (2011). Molecular mapping of general anesthetic sites in a voltage-gated ion channel. Biophys. J. *101*, 1613–1622.

Barber, A.F., Carnevale, V., Klein, M.L., Eckenhoff, R.G., and Covarrubias, M. (2014). Modulation of a voltage-gated Na$^+$ channel by sevoflurane involves multiple sites and distinct mechanisms. Proc. Natl. Acad. Sci. USA *111*, 6726–6731.

Berka, K., Hanák, O., Sehnal, D., Banás, P., Navrátilová, V., Jaiswal, D., Ionescu, C.M., Svobodová Vareková, R., Kočа, J., and Otyepka, M. (2012). MOLEonline 2.0: interactive web-based analysis of biomacromolecular channels. Nucleic Acids Res. 40, W222–W227.

Bertaccini, E.J., Yoluk, O., Lindahl, E.R., and Trudell, J.R. (2013). Assessment of homology templates and an anesthetic binding site within the γ-aminobutyric acid receptor. Anesthesiology 119, 1087–1095.

Bertrand, S., Devillers-Thiéry, A., Palma, E., Buisson, B., Edelstein, S.J., Corringer, P.J., Changeux, J.P., and Bertrand, D. (1997). Paradoxical allosteric effects of competitive inhibitors on neuronal α7 nicotinic receptor mutants. Neuroreport 8, 3591–3596.

Blanc, E., Roversi, P., Vonrhein, C., Flensburg, C., Lea, S.M., and Bricogne, G. (2004). Refinement of severely incomplete structures with maximum likelihood in BUSTER-TNT. Acta Crystallogr. D Biol. Crystallogr. 60, 2210–2221.

Bocquet, N., Prado de Carvalho, L., Cartaud, J., Neyton, J., Le Poupon, C., Taly, A., Grutter, T., Changeux, J.P., and Corringer, P.J. (2007). A prokaryotic proton-gated ion channel from the nicotinic acetylcholine receptor family. Nature 445, 116–119.

Bocquet, N., Nury, H., Baaden, M., Le Poupon, C., Changeux, J.P., Delarue, M., and Corringer, P.J. (2009). X-ray structure of a pentameric ligand-gated ion channel in an apparently open conformation. Nature 457, 111–114.

Borghese, C.M., Ruiz, C.I., Lee, U.S., Cullins, M.A., Bertaccini, E.J., Trudell, J.R., and Harris, R.A. (2016). Identification of an inhibitory alcohol binding site in GABA_A ρ1 receptors. ACS Chem. Neurosci. 7, 100–108.

Brünger, A.T. (1992). Free R value: a novel statistical quantity for assessing the accuracy of crystal structures. Nature 355, 472–475.

Changeux, J.P. (2013a). 50 years of allosteric interactions: the twists and turns of the models. Nat. Rev. Mo.l Cell Biol. 14, 819–829.

Changeux, J.P. (2013b). The concept of allosteric modulation: an overview. Drug Discov. Today. Technol. 10, e223–e228.

Changeux, J.P., and Christopoulos, A. (2016). Allosteric modulation as a unifying mechanism for receptor function and regulation. Cell 166, 1084–1102.

Chen, Q., Kinde, M.N., Arjunan, P., Wells, M.M., Cohen, A.E., Xu, Y., and Tang, P. (2015). Direct pore binding as a mechanism for isoflurane inhibition of the pentameric ligand-gated ion channel ELIC. Sci. Rep. 5, 13833.

Chen, Q., Wells, M.M., Tillman, T.S., Kinde, M.N., Cohen, A., Xu, Y., and Tang, P. (2017). Structural basis of alcohol inhibition of the pentameric ligand-gated ion channel ELIC. Structure 25, 180–187.

Chiara, D.C., Gill, J.F., Chen, Q., Tillman, T., Dailey, W.P., Eckenhoff, R.G., Xu, Y., Tang, P., and Cohen, J.B. (2014). Photoaffinity labeling the propofol binding site in GLIC. Biochemistry 53, 135–142.

Collaborative Computational Project, Number 4 (1994). The CCP4 suite: programs for protein crystallography. Acta Crystallogr. D Biol. Crystallogr. 50, 760–763.

Davis, I.W., Leaver-Fay, A., Chen, V.B., Block, J.N., Kapral, G.J., Wang, X., Murray, L.W., Arendall, W.B., 3rd, Snoeyink, J., Richardson, J.S., and Richardson, D.C. (2007). MolProbity: all-atom contacts and structure validation for proteins and nucleic acids. Nucleic Acids Res. 35, W375–W383.

Du, J., Lü, W., Wu, S., Cheng, Y., and Gouaux, E. (2015). Glycine receptor mechanism elucidated by electron cryo-microscopy. Nature 526, 224–229.

Flood, P., Ramirez-Latorre, J., and Role, L. (1997). α 4 β 2 neuronal nicotinic acetylcholine receptors in the central nervous system are inhibited by isoflurane and propofol, but α 7-type nicotinic acetylcholine receptors are unaffected. Anesthesiology 86, 859–865.

Fourati, Z., Ruza, R.R., Laverty, D., Drège, E., Delarue-Cochin, S., Joseph, D., Koehl, P., Smart, T., and Delarue, M. (2017). Barbiturates bind in the GLIC ion channel pore and cause inhibition by stabilizing a closed state. J. Biol. Chem. 292, 1550–1558.

Franks, N.P. (2006). Molecular targets underlying general anaesthesia. Br. J. Pharmacol. 147 (Suppl 1), S72–S81.

Franks, N.P. (2015). Structural comparisons of ligand-gated ion channels in open, closed, and desensitized states identify a novel propofol-binding site on mammalian γ-aminobutyric acid type A receptors. Anesthesiology 122, 787–794.

Gao, J., Wu, X.H., Dong, W.L., and Wang, S.Q. (2013). A series of propofol analogs design by targeting pentameric ligand-gated ion channel in silico method. Protein Pept. Lett. 20, 1238–1245.

Ghosh, B., Satyshur, K.A., and Czajkowski, C. (2013). Propofol binding to the resting state of the gloeobacter violaceus ligand-gated ion channel (GLIC) induces structural changes in the inter- and intrasubunit transmembrane domain (TMD) cavities. J. Biol. Chem. 288, 17420–17431.

Gonzalez-Gutierrez, G., Cuello, L.G., Nair, S.K., and Grosman, C. (2013). Gating of the proton-gated ion channel from Gloeobacter violaceus at pH 4 as revealed by X-ray crystallography. Proc. Natl. Acad. Sci. USA 110, 18716–18721.

Gregoret, L.M., Rader, S.D., Fletterick, R.J., and Cohen, F.E. (1991). Hydrogen bonds involving sulfur atoms in proteins. Proteins 9, 99–107.

Hassaine, G., Deluz, C., Grasso, L., Wyss, R., Tol, M.B., Hovius, R., Graff, A., Stahlberg, H., Tomizaki, T., Desmyter, A., et al. (2014). X-ray structure of the mouse serotonin 5-HT_3 receptor. Nature 512, 276–281.

Heusser, S.A., Howard, R.J., Borghese, C.M., Cullins, M.A., Broemstrup, T., Lee, U.S., Lindahl, E., Carlsson, J., and Harris, R.A. (2013). Functional validation of virtual screening for novel agents with general anesthetic action at ligand-gated ion channels. Mol. Pharmacol. 84, 670–678.

Heusser, S.A., Yoluk, Ö., Klement, G., Riederer, E.A., Lindahl, E., and Howard, R.J. (2016). Functional characterization of neurotransmitter activation and modulation in a nematode model ligand-gated ion channel. J. Neurochem. 138, 243–253.

Hibbs, R.E., and Gouaux, E. (2011). Principles of activation and permeation in an anion-selective Cys-loop receptor. Nature 474, 54–60.

Hilf, R.J., and Dutzler, R. (2009). Structure of a potentially open state of a proton-activated pentameric ligand-gated ion channel. Nature 457, 115–118.

Hilf, R.J., Bertozzi, C., Zimmermann, I., Reiter, A., Trauner, D., and Dutzler, R. (2010). Structural basis of open channel block in a prokaryotic pentameric ligand-gated ion channel. Nat. Struct. Mol. Biol. 17, 1330–1336.

Howard, R.J., Murail, S., Ondricek, K.E., Corringer, P.J., Lindahl, E., Trudell, J.R., and Harris, R.A. (2011). Structural basis for alcohol modulation of a pentameric ligand-gated ion channel. Proc. Natl. Acad. Sci. USA 108, 12149–12154.

Howard, R.J., Trudell, J.R., and Harris, R.A. (2014). Seeking structural specificity: direct modulation of pentameric ligand-gated ion channels by alcohols and general anesthetics. Pharmacol. Rev. 66, 396–412.

Huang, X., Chen, H., Michelsen, K., Schneider, S., and Shaffer, P.L. (2015). Crystal structure of human glycine receptor-α3 bound to antagonist strychnine. Nature 526, 277–280.

Jayakar, S.S., Dailey, W.P., Eckenhoff, R.G., and Cohen, J.B. (2013). Identification of propofol binding sites in a nicotinic acetylcholine receptor with a photoreactive propofol analog. J. Biol. Chem. 288, 6178–6189.

Jayakar, S.S., Zhou, X., Chiara, D.C., Dostalova, Z., Savechenkov, P.Y., Bruzik, K.S., Dailey, W.P., Miller, K.W., Eckenhoff, R.G., and Cohen, J.B. (2014). Multiple propofol-binding sites in a γ-aminobutyric acid type A receptor (GABAAR) identified using a photoreactive propofol analog. J. Biol. Chem. 289, 27456–27468.

Jayakar, S.S., Zhou, X., Savechenkov, P.Y., Chiara, D.C., Desai, R., Bruzik, K.S., Miller, K.W., and Cohen, J.B. (2015). Positive and negative allosteric modulation of an α1β3γ2 γ-Aminobutyric Acid Type A (GABAA) receptor by binding to a site in the transmembrane domain at the γ+-β− interface. J. Biol. Chem. 290, 23432–23446.

Johnson, W.D., 2nd, Howard, R.J., Trudell, J.R., and Harris, R.A. (2012). The TM2 6′ position of GABA(A) receptors mediates alcohol inhibition. J. Pharmacol. Exp. Ther. 340, 445–456.

Joseph, T.T., and Mincer, J.S. (2016). Common internal allosteric network links anesthetic binding sites in a pentameric ligand-gated ion channel. PLoS ONE 11, e0158795.

Jurd, R., Arras, M., Lambert, S., Drexler, B., Siegwart, R., Crestani, F., Zaugg, M., Vogt, K.E., Ledermann, B., Antkowiak, B., and Rudolph, U. (2003). General anesthetic actions *in vivo* strongly attenuated by a point mutation in the GABA($_A$) receptor β3 subunit. FASEB J. *17*, 250–252.

Kabsch, W. (2010). XDS. Acta Crystallogr. D Biol. Crystallogr. *66*, 125–132.

Laurent, B., Murail, S., Shahsavar, A., Sauguet, L., Delarue, M., and Baaden, M. (2016). Sites of anesthetic inhibitory action on a cationic ligand-gated ion channel. Structure *24*, 595–605.

LeBard, D.N., Hénin, J., Eckenhoff, R.G., Klein, M.L., and Brannigan, G. (2012). General anesthetics predicted to block the GLIC pore with micromolar affinity. PLoS Comput. Biol. *8*, e1002532.

Lev, B., Murail, S., Poitevin, F., Cromer, B.A., Baaden, M., Delarue, M., and Allen, T.W. (2017). String method solution of the gating pathways for a pentameric ligand-gated ion channel. Proc. Natl. Acad. Sci. USA *114*, E4158–E4167.

Lynagh, T., and Laube, B. (2014). Opposing effects of the anesthetic propofol at pentameric ligand-gated ion channels mediated by a common site. J. Neurosci. *34*, 2155–2159.

Lynagh, T., Kunz, A., and Laube, B. (2013). Propofol modulation of α1 glycine receptors does not require a structural transition at adjacent subunits that is crucial to agonist-induced activation. ACS Chem. Neurosci. *4*, 1469–1478.

Meng, E.C., Pettersen, E.F., Couch, G.S., Huang, C.C., and Ferrin, T.E. (2006). Tools for integrated sequence-structure analysis with UCSF Chimera. BMC Bioinformatics *7*, 339.

Menny, A., Lefebvre, S.N., Schmidpeter, P.A., Drège, E., Fourati, Z., Delarue, M., Edelstein, S.J., Nimigean, C.M., Joseph, D., and Corringer, P.J. (2017). Identification of a pre-active conformation of a pentameric channel receptor. eLife *6*, e23955.

Miller, P.S., and Aricescu, A.R. (2014). Crystal structure of a human GABA$_A$ receptor. Nature *512*, 270–275.

Morales-Perez, C.L., Noviello, C.M., and Hibbs, R.E. (2016). X-ray structure of the human α4β2 nicotinic receptor. Nature *538*, 411–415.

Murshudov, G.N., Skubák, P., Lebedev, A.A., Pannu, N.S., Steiner, R.A., Nicholls, R.A., Winn, M.D., Long, F., and Vagin, A.A. (2011). REFMAC5 for the refinement of macromolecular crystal structures. Acta Crystallogr. D Biol. Crystallogr. *67*, 355–367.

Nirthanan, S., Garcia, G., 3rd, Chiara, D.C., Husain, S.S., and Cohen, J.B. (2008). Identification of binding sites in the nicotinic acetylcholine receptor for TDBzl-etomidate, a photoreactive positive allosteric effector. J. Biol. Chem. *283*, 22051–22062.

Nury, H., Van Renterghem, C., Weng, Y., Tran, A., Baaden, M., Dufresne, V., Changeux, J.P., Sonner, J.M., Delarue, M., and Corringer, P.J. (2011). X-ray structures of general anaesthetics bound to a pentameric ligand-gated ion channel. Nature *469*, 428–431.

Nys, M., Kesters, D., and Ulens, C. (2013). Structural insights into Cys-loop receptor function and ligand recognition. Biochem. Pharmacol. *86*, 1042–1053.

Olsen, R.W., Li, G.D., Wallner, M., Trudell, J.R., Bertaccini, E.J., Lindahl, E., Miller, K.W., Alkana, R.L., and Davies, D.L. (2014). Structural models of ligand-gated ion channels: sites of action for anesthetics and ethanol. Alcohol. Clin. Exp. Res. *38*, 595–603.

Prevost, M.S., Sauguet, L., Nury, H., Van Renterghem, C., Huon, C., Poitevin, F., Baaden, M., Delarue, M., and Corringer, P.J. (2012). A locally closed conformation of a bacterial pentameric proton-gated ion channel. Nat. Struct. Mol. Biol. *19*, 642–649.

Sauguet, L., Howard, R.J., Malherbe, L., Lee, U.S., Corringer, P.J., Harris, R.A., and Delarue, M. (2013a). Structural basis for potentiation by alcohols and anaesthetics in a ligand-gated ion channel. Nat. Commun. *4*, 1697.

Sauguet, L., Poitevin, F., Murail, S., Van Renterghem, C., Moraga-Cid, G., Malherbe, L., Thompson, A.W., Koehl, P., Corringer, P.J., Baaden, M., and Delarue, M. (2013b). Structural basis for ion permeation mechanism in pentameric ligand-gated ion channels. EMBO J. *32*, 728–741.

Sauguet, L., Shahsavar, A., Poitevin, F., Huon, C., Menny, A., Nemecz, À., Haouz, A., Changeux, J.P., Corringer, P.J., and Delarue, M. (2014). Crystal structures of a pentameric ligand-gated ion channel provide a mechanism for activation. Proc. Natl. Acad. Sci. USA *111*, 966–971.

Sauguet, L., Fourati, Z., Prangé, T., Delarue, M., and Colloc'h, N. (2016). Structural basis for xenon inhibition in a cationic pentameric ligand-gated ion channel. PLoS ONE *11*, e0149795.

Smart, T.G., and Paoletti, P. (2012). Synaptic neurotransmitter-gated receptors. Cold Spring Harb. Perspect. Biol. *4*, a009662.

Spurny, R., Billen, B., Howard, R.J., Brams, M., Debaveye, S., Price, K.L., Weston, D.A., Strelkov, S.V., Tytgat, J., Bertrand, S., et al. (2013). Multisite binding of a general anesthetic to the prokaryotic pentameric Erwinia chrysanthemi ligand-gated ion channel (ELIC). J. Biol. Chem. *288*, 8355–8364.

Stewart, D.S., Pierce, D.W., Hotta, M., Stern, A.T., and Forman, S.A. (2014). Mutations at beta N265 in γ-aminobutyric acid type A receptors alter both binding affinity and efficacy of potent anesthetics. PLoS ONE *9*, e111470.

Süel, G.M., Lockless, S.W., Wall, M.A., and Ranganathan, R. (2003). Evolutionarily conserved networks of residues mediate allosteric communication in proteins. Nat. Struct. Biol. *10*, 59–69.

Tillman, T., Cheng, M.H., Chen, Q., Tang, P., and Xu, Y. (2013). Reversal of ion-charge selectivity renders the pentameric ligand-gated ion channel GLIC insensitive to anaesthetics. Biochem. J. *449*, 61–68.

Violet, J.M., Downie, D.L., Nakisa, R.C., Lieb, W.R., and Franks, N.P. (1997). Differential sensitivities of mammalian neuronal and muscle nicotinic acetylcholine receptors to general anesthetics. Anesthesiology *86*, 866–874.

Weng, Y., Yang, L., Corringer, P.J., and Sonner, J.M. (2010). Anesthetic sensitivity of the *Gloeobacter violaceus* proton-gated ion channel. Anesth. Analg. *110*, 59–63.

Wick, M.J., Mihic, S.J., Ueno, S., Mascia, M.P., Trudell, J.R., Brozowski, S.J., Ye, Q., Harrison, N.L., and Harris, R.A. (1998). Mutations of gamma-aminobutyric acid and glycine receptors change alcohol cutoff: evidence for an alcohol receptor? Proc. Natl. Acad. Sci. USA *95*, 6504–6509.

Yip, G.M.S., Chen, Z.-W., Edge, C.J., Smith, E.H., Dickinson, R., Hohenester, E., Townsend, R.R., Fuchs, K., Sieghart, W., Evers, A.S., and Franks, N.P. (2013). A propofol binding site on mammalian GABA$_A$ receptors identified by photolabeling. Nat. Chem. Biol. *9*, 715–720.

Zamyatnin, A.A. (1972). Protein volume in solution. Prog. Biophys. Mol. Biol. *24*, 107–123.

Ziemba, A.M., and Forman, S.A. (2016). Correction for inhibition leads to an allosteric co-agonist model for pentobarbital modulation and activation of α1β3γ2L GABA$_A$ receptors. PLoS ONE *11*, e0154031.